Short-pulse cross-phase modulation in an electromagnetically-induced-transparency medium

Amir Feizpour,[1,*] Greg Dmochowski,[1] and Aephraim M. Steinberg[1,2]
[1]*Centre for Quantum Information and Quantum Control and Institute for Optical Sciences, Department of Physics, University of Toronto, 60 St. George Street, Toronto, Ontario M5S 1A7, Canada*
[2]*Canadian Institute For Advanced Research, 180 Dundas Street West, Toronto, Ontario M5G 1Z8, Canada*
(Received 27 May 2015; published 19 January 2016)

Electromagnetically induced transparency (EIT) has been proposed as a way to greatly enhance cross-phase modulation, with the possibility of leading to few-photon-level optical nonlinearities [Schmidt and Imamoglu, Opt. Lett. **21**, 1936 (1996)]. This enhancement grows as the transparency window width, Δ_{EIT}, is narrowed. Decreasing Δ_{EIT}, however, has been shown to increase the response time of the nonlinear medium. This suggests that, for a given pulse duration, the nonlinearity would diminish once the window width became narrower than this pulse bandwidth. We show that this is not the case: the peak phase shift saturates but does not decrease. We show that in the regimes of most practical interest—narrow EIT windows perturbed by short signal pulses—the enhancement offered by EIT is not only in the magnitude of the nonlinear phase shift but also in its increased duration. That is, for the case of signal pulses much shorter (temporally) than the inverse EIT bandwidth, the narrow window serves to prolong the effect of the passing signal pulse, leading to an integrated phase shift that grows linearly with $1/\Delta_{\mathrm{EIT}}$; this continued growth of the integrated phase shift improves the detectability of the phase shift, in principle, without bound. For many purposes, it is this detectability which is of more interest than the absolute magnitude of the peak phase shift. We present analytical expressions based on a linear time-invariant model that accounts for the temporal behavior of the cross-phase modulation for several parameter ranges of interest. We conclude that in order to optimize the detectability of the EIT-based cross-phase shift, one should use the narrowest possible EIT window and a signal pulse that is as broadband as the excited-state linewidth and detuned by half a linewidth.

DOI: 10.1103/PhysRevA.93.013834

I. INTRODUCTION

While photonic qubits are ideal candidates for quantum information storage and transmission, an efficient and scalable method for processing optical quantum information has yet to be demonstrated. The weakly interacting nature of light, which makes photonic qubits robust against decoherence, also renders photons poor candidates for information processing since (nonlinear) interactions are at the heart of logic gate operations.

A large enough optical nonlinearity at the quantum level can pave the way for numerous applications, including low-light-level switching [1], quantum nondemolition measurements [2], quantum teleportation [3], and quantum logic gates [4]. However, naturally occurring nonlinear optical coefficients are insufficient for these applications. Several approaches have been taken to tackling the problem of very weak nonlinearities, including the use of photonic crystal fibers [5], Rydberg atoms [6–9], atoms in hollow-core fibers [10], single atoms coupled to microresonators [11], and a proposal to amplify the magnitude of existing nonlinear optical effects [12]. Schmidt and Imamoglu proposed a scheme [13] based on electromagnetically induced transparency (EIT) [14] which allowed for "giant," resonantly enhanced optical nonlinearities while simultaneously eliminating absorption; see [15–17] for examples of the experimental realization of this scheme. While offering an orders-of-magnitude increase in the interaction strength, which scales inversely with the transparency window width, this work was based on a single-mode treatment and did not consider practical details of the effect in the presence of pulsed light fields.

This paper investigates whether the enhancement offered by the original proposal persists for experimentally realistic conditions which call for broadband signal pulses, narrow EIT windows, and optically thick media. Here we show that in the regime of narrow transparency windows perturbed by short signal pulses, the peak cross-phase shift (XPS) saturates without shrinking, contrary to previous fears, and the duration of the effect grows as the window becomes narrower. While the rise time of the EIT-enhanced XPS is determined by the signal pulse duration, τ_s, its fall is given by the inverse EIT window width, resulting in an integrated nonlinear phase shift that continues to scale inversely with the window width even for $\Delta_{\mathrm{EIT}} \ll 1/\tau_S$. In addition, while step-response analysis showed that increasing the optical density (OD) of the medium increased the rise time of the nonlinearity, here again we show that the rise time is unaffected when pulsed signal fields are considered; higher ODs merely result in an elongation of the XPS, which can aid in the detection of this effect. The results reported in this paper disprove some of the previously believed dependences for EIT-enhanced optical nonlinearity and present the correct scalings for experimentally relevant parameter regimes.

There have been several multimode treatments of EIT, which examine the transients due to switching on optical fields [18,19] as well as of sudden changes in two-photon (Raman) resonance [20,21]. In addition, the transient properties of the associated nonlinearities, both absorptive (photon switching) [22,23] and dispersive (cross-Kerr effect) [24–28], have since been investigated. In particular, it was found that the rise time of the cross-phase modulation, that is, the time required for

*feizpour@physics.utoronto.ca

the phase of the probe field to reach its new steady-state value in response to a step-function signal field, is inversely proportional to the EIT window width, Δ_{EIT}. While narrower EIT windows provide a larger steady-state phase shift, more time is needed to reach this steady state. In [26,28] the authors suggest that there is an inherent limitation to EIT-enhanced cross-phase modulation schemes; they directly generalized the step-response results to pulsed signal fields and concluded that using EIT to increase the nonlinearity also renders the medium slow to respond. However, this approach is not valid for the case of short signal pulses and an appropriate study of this relevant regime is missing.

Early schemes for optical quantum information processing required very large (of the order of π) XPSs [29]. As this has proven to be experimentally out of reach in single-pass geometries so far, more recent proposals have replaced the need for such large phase shifts with the less demanding requirement of any XPS detectable in a single shot [4]. In this proposal, each qubit single photon interacts individually with the same classical electromagnetic field ("bus"). A subsequent phase measurement on this bus projects the two qubits into an entangled state up to a local correction. The crucial step here is to be able to *detect* the nonlinear phase shift of the single photon on the classical beam in a single shot. In order to improve the detectability of the phase shift, one usually integrates the effect over its duration. In other words, not only the peak size of the nonlinear phase shift but also its duration plays an important role. We, therefore, study both the peak and the integrated nonlinear phase shift. It is important to note that no experiment so far has been able to demonstrate a single-shot measurement of a nonlinear phase shift due to a single photon.

We begin by introducing in Sec. II A the rigorous mathematical approach (based on the Maxwell-Bloch equations) used to study this light-matter interaction. In Sec. II B we show that the dynamics of these XPSs can be understood in terms of a linear time-invariant (LTI) model [30]. The intensity of the signal field and the phase of the probe field can be thought of as the "drive" and "response" of a linear system, respectively. Analytical expressions based on an LTI system response accurately model the behavior of the nonlinear interaction in most regimes of interest. The results of these two approaches are discussed in Sec. III, where we describe behavior of EIT-enhanced XPS with pulsed signal fields including its dependence on various parameters of interest such as the transparency window width and the signal pulse duration. Finally, in Sec. III C we discuss how propagation in an optically thick medium affects EIT-enhanced cross-phase modulation. Throughout, we compare the predictions of an LTI model and the numerical solutions of the complete system density matrix and discuss the range of validity of such a model.

II. N SCHEME

Consider the atomic level scheme shown in Fig. 1, in which continuous-wave in-phase probe and coupling fields form a three-level Lambda system. If the two-photon resonance condition is satisfied, i.e., $\delta = \Delta_p - \Delta_c = 0$, and the coupling field is strong enough, $\Omega_c^2 \gg \Gamma\gamma$, then destructive interference of multiple excitation pathways causes the medium to become transparent to the probe light. That is, the interaction of the

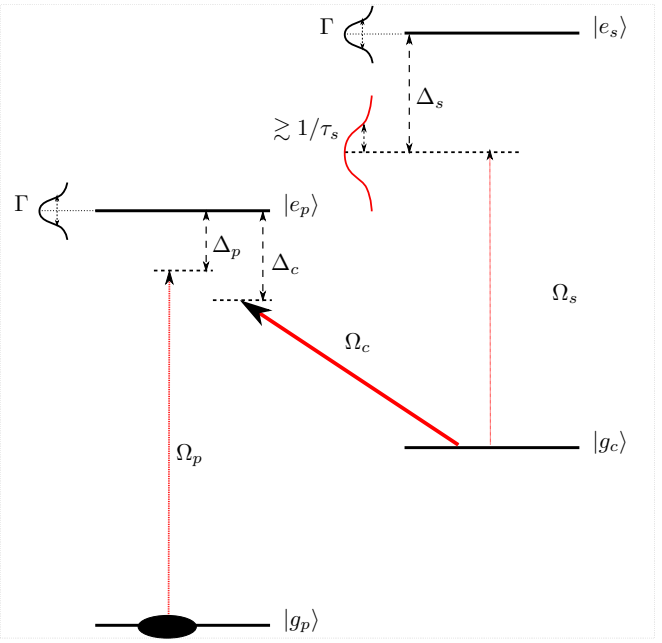

FIG. 1. Level structure for the simplest EIT-enhanced cross-Kerr effect, the so-called N scheme. Here, Ω_p and Ω_c are the Rabi frequencies of the (continuous-wave) probe and coupling fields; Ω_s is the peak Rabi frequency of the signal field, which is a Gaussian pulse of length τ_s; Γ is the excited-state decay rate; and γ is the ground-state dephasing rate.

probe and coupling fields with the medium results in new atomic eigenstates, one of which (the so-called dark state) is decoupled from the optical fields. Atomic population is pumped into this dark state, where it remains, at a rate of $R = \Omega_c^2\Gamma/2(4\Delta^2 + \Gamma^2)$, where $\Delta = (\Delta_p + \Delta_c)/2$. The steady-state spectral width (FWHM) of the EIT window is determined by this pumping rate along with the ground-state dephasing rate according to $\Delta_{\mathrm{EIT}} = 2(R + \gamma)$ [27]. The presence of the signal field inside the medium completes the "N scheme," serving to perturb the ground-state coherence created by the Lambda system in two ways: first, the scattering of the signal photons from the excited state $|e_s\rangle$ dephases the ground-state coherence at the rate of $\Omega_s^2\Gamma/4\Delta_s^2$; second, the Stark shift caused by the signal pulse, $\Delta_{\mathrm{ACS}} = \Omega_s^2/4\Delta_s$, detunes the system out of two-photon resonance and causes the probe field to experience a different refractive index, thereby acquiring an XPS. The signal detuning can be made large enough compared to both the excited-state linewidth and the bandwidth of the signal pulse that the first contribution is negligible and only the Stark shift perturbs the system significantly. If this Stark shift, Δ_{ACS}, is smaller than the EIT window width, Δ_{EIT}, then the phase shift that the probe experiences is linear in Δ_{ACS} and, in turn, linear in the intensity of the signal field, $|\Omega_s|^2$. This is the regime in which the nonlinear interaction between the signal and the probe can be considered a cross-Kerr effect.

A. Maxwell-Bloch model

The Hamiltonian describing the interactions in Fig. 1 (in a rotating frame and using the rotating-wave approximation)

is

$$H = \frac{\hbar}{2}\begin{pmatrix} 0 & 0 & \Omega_p & 0 \\ 0 & 2\delta & \Omega_c & \Omega_s \\ \Omega_p^* & \Omega_c^* & 2\Delta_p & 0 \\ 0 & \Omega_s^* & 0 & 2(\Delta_s+\delta) \end{pmatrix}, \tag{1}$$

where $\Omega_i = -\vec{\mu}\cdot\vec{E}_i/\hbar$ is the Rabi frequency and E_i is the electric field for $i = p,c,s$; $\vec{\mu}$ is the dipole matrix element of the transition. We can find the dynamics of the system by solving the Maxwell-Bloch equations,

$$\begin{aligned}
\partial_t\Omega_p + c\partial_z\Omega_p &= igN(z)S_p(z,t),\\
\partial_t\Omega_c + c\partial_z\Omega_c &= igN(z)S_c(z,t),\\
\partial_t\Omega_s + c\partial_z\Omega_s &= igN(z)S_s(z,t),\\
\partial_t S_p &= (i\Delta_p - \Gamma/2)S_p(z,t) + i\tfrac{1}{2}\Omega_p(z,t) + i\tfrac{1}{2}\Omega_c(z,t)S_{gg}(z,t),\\
\partial_t S_s &= (i\Delta_s - \Gamma/2)S_s(z,t) - i\tfrac{1}{2}\Omega_c(z,t)S_{ee}(z,t),\\
\partial_t S_c &= (i\Delta_c - \Gamma/2)S_c(z,t) - i\tfrac{1}{2}\Omega_s(z,t)S^*_{ee}(z,t) + i\tfrac{1}{2}\Omega_p(z,t)S^*_{gg}(z,t),\\
\partial_t S_{gg} &= (i\delta - \gamma)S_{gg}(z,t) + i\tfrac{1}{2}\Omega^*_c(z,t)S_p(z,t) - i\tfrac{1}{2}\Omega_p(z,t)S^*_c(z,t) + i\tfrac{1}{2}\Omega^*_s(z,t)S_{ge}(z,t),\\
\partial_t S_{ee} &= (i(\Delta_s - \Delta_c) - \Gamma/2)S_{ee}(z,t) + i\tfrac{1}{2}\Omega_s(z,t)S^*_c(z,t) - i\tfrac{1}{2}\Omega^*_p(z,t)S_{ge}(z,t) - i\tfrac{1}{2}\Omega^*_c(z,t)S_s(z,t),\\
\partial_t S_{ge} &= (i(\Delta_s + \Delta_p - \Delta_c) - \Gamma/2)S_{ge}(z,t) - i\tfrac{1}{2}\Omega_p(z,t)S_{ee}(z,t) + i\tfrac{1}{2}\Omega_s(z,t)S_{gg}(z,t),
\end{aligned} \tag{2}$$

which encapsulate the dynamics of both the atomic system and the electromagnetic fields. In Eqs. (2), c is the speed of light; $N(z)$ is the atom density; $S_p = \mathrm{Tr}(\rho|g_p\rangle\langle e_p|)$, $S_c = \mathrm{Tr}|(\rho|g_c\rangle\langle e_p|)$, and $S_s = \mathrm{Tr}(\rho|g_c\rangle\langle e_s|)$ are the probe, coupling, and signal transition coherences, respectively; $S_{gg} = \mathrm{Tr}(\rho|g_p\rangle\langle g_c|)$, $S_{ee} = \mathrm{Tr}(\rho|e_p\rangle\langle e_s|)$, and $S_{ge} = \mathrm{Tr}(\rho|g_p\rangle\langle e_s|)$ are the coherences between the two ground states, between the two excited states, and between the probe ground state and the signal excited state, respectively; ρ is the atomic density matrix; and $g = \omega_0\mu^2/\epsilon_0\hbar$ is the light-matter coupling constant, where ω_0 is the center frequency of the electromagnetic field. For the purposes of this paper ω_0 and μ are taken to be constants and equal for all transitions. In deriving the above equations of motion, it is assumed that all optical fields are weak enough that the population remains completely in the probe ground state, $|g_p\rangle$. Therefore, to first order in electric fields, the equations of motion for populations can be neglected. We assume a Gaussian distribution for atom density and set both one- and two-photon detunings to 0, $\Delta_p = 0$, and $\Delta_c - \Delta_p = 0$, respectively. In addition, the probe and coupling fields are assumed to be continuous wave (pulses with durations much longer than the simulation time), while the signal pulse is taken to be Gaussian with an rms duration of τ_s. The probe and coupling fields have to be long enough to encompass all of the dynamics of the system, especially any potentially long-lasting transient behavior. Note that the OD of a transition is given by $d_0 = (2g/c\Gamma)\int N(z)dz = \sigma_{\mathrm{at}}\int N(z)dz$ where σ_{at} is the interaction cross section.

The equations of motion, Eq. (2), can be solved using approximate analytical methods [27] or numerical techniques. We take the latter route, using a first-order difference method to discretize the spatial coordinate and then the fourth-order Runge-Kutta method to take the time integral, which yields the solution to the density matrix of the combined light-matter system for different sets of parameter choices. First, however, we present an alternate and simpler approach to modeling the dynamics as an LTI system. The results in Sec. III compare and contrast these two approaches.

B. Linear time-invariant model

Here we present a model for the dynamics of the cross-Kerr interaction, which abstracts the underlying nonlinearities and treats the probe phase as the "output" of an LTI system whose behavior is affected by an independent, potentially time-varying, "driving" signal-field intensity. The impulse response characterizing this linear system may be obtained by direct differentiation of the system's step response. This step response is precisely what has been reported in previous transient studies of EIT-enhanced XPS [27]. There it was shown that, when the Stark shift is smaller than the EIT window width, the rise time of the XPS is $\tau = (1 + d/4)/(R + \gamma)$, where $d = d_0R/(R + \gamma)$ is the depth of the transparency (the difference in the OD seen by the on-resonance probe without and the OD with a resonant coupling beam). We, therefore, take the step response, $\mathcal{S}(t)$, to have an exponential shape,

$$\mathcal{S}(t) = \frac{\phi^{\mathrm{ss}}}{|\Omega|^2}\Theta(t)(1 - \exp(-t/\tau)), \tag{3}$$

where ϕ^{ss} is the steady-state XPS for a weak signal field of intensity $|\Omega|^2$, and $\Theta(t)$ is the Heaviside step function. It is important to note that the shape of the response in an optically thick medium deviates from the exponential form. For simplicity, we first consider optically thin media, leaving the details of optically thick samples to Sec. III C. The steady-state phase shift, ϕ^{ss}, as predicted by single-mode and

step-response treatments, is

$$\begin{aligned}\phi^{\rm ss} &= \Delta_{\rm ACS}\frac{\omega_0}{2c}\int dz\,\frac{\partial\chi_{\rm pr}(z)}{\partial\Delta_p}\bigg|_{\Delta_c=0,\ \delta=0}\\ &= \Delta_{\rm ACS}\frac{\omega_0}{2c}\frac{4d^2}{\hbar\epsilon_0}\frac{\Omega_c^2}{\left(2\gamma\Gamma+\Omega_c^2\right)^2}\int N(z)dz\\ &= \Delta_{\rm ACS}d_0\Gamma\frac{\Omega_c^2}{\left(2\gamma\Gamma+\Omega_c^2\right)^2} = \Delta_{\rm ACS}\frac{d}{\Delta_{\rm EIT}},\end{aligned}\tag{4}$$

where $\chi_{\rm pr}$ is the steady-state susceptibility of the probe transition [14], $\Delta_{\rm ACS} = -|\Omega|^2/4\Delta_s$ is the ground-state Stark shift for $\Delta_s \gg \Gamma$, and $d/\Delta_{\rm EIT}$ is proportional to the slope of the refractive index with respect to the detuning seen by the probe field. The impulse response can be obtained by differentiating the above step response:

$$\mathcal{I}(t) = \frac{\partial\mathcal{S}(t)}{\partial t} = \frac{\phi^{\rm ss}}{|\Omega|^2\tau}\Theta(t)\exp(-t/\tau).\tag{5}$$

Let us now investigate the behavior of this system in response to a Gaussian signal pulse. We describe the pulse by its time-dependent Rabi frequency,

$$\Omega_s(t) = \Omega_{0,s}\left(\frac{1}{2\tau_s^2\Gamma^2}\right)^{1/4}\exp\left(-t^2/4\tau_s^2\right).\tag{6}$$

With applications of single-photon nonlinearities in mind, we consider a fixed number of signal photons, $n_{\rm ph}$, constraining the pulse energy,

$$E = \left(\sqrt{\pi}\frac{\Omega_{0,s}^2}{\Gamma^2}\frac{A}{\sigma_{\rm at}}\right)\hbar\omega_0 = n_{\rm ph}\hbar\omega_0,\tag{7}$$

where A is the transverse area of the signal pulse. Assuming linearity, the temporal profile of the XPS is the convolution of the impulse response and the intensity profile of the signal pulse,

$$\begin{aligned}\phi(t) &= |\Omega_s(t)|^2 * \mathcal{I}(t)\\ &= \frac{\phi_0 n_{\rm ph}}{2\tau}e^{\tau_s^2/2\tau^2}\\ &\quad\times\exp(-t/\tau)(1+\mathrm{erf}(t/\sqrt{2}\tau_s - \tau_s/\sqrt{2}\tau)),\end{aligned}\tag{8}$$

where $\mathrm{erf}(x) = 2/\sqrt{\pi}\int_0^x dx'\exp(-x'^2)$ is the error function, $*$ indicates convolution, and

$$\phi_0 = \frac{\Gamma}{-4\Delta_s}\frac{\sigma_{\rm at}}{A}\frac{d}{\Delta_{\rm EIT}}\tag{9}$$

is the integrated XPS per signal photon. The temporal profile of the XPS predicted by the LTI model, Eq. (8), suggests that there are two time scales involved: the response time of the EIT medium, τ, and the signal pulse duration, τ_s. Initially, when $t \ll \tau$, the error function term alone dictates the temporal shape, having a time scale given by τ_s. The rise of the phase shift always mimics the envelope of the signal pulse, irrespective of τ. For later times, however, the temporal shape of the phase shift is given by a combination of the signal pulse duration and the response time of the EIT medium. In the limiting case of $\tau_s \gg \tau$ (when the signal pulse is much longer than the response time of the medium), the probe phase follows the signal pulse envelope. This corresponds to a quasi-steady-state scenario where the atomic coherences are able to follow the change in two-photon detuning arising from the signal field. At the other extreme, when $\tau_s \ll \tau$, the phase of the probe field rises quickly due to the short signal pulse and then relaxes to its original steady-state value on a time scale given by τ alone. This corresponds to a short impulse perturbing the system momentarily, leaving the atomic coherences to build back up once it passes. For intermediate cases, the phase decays on a time scale which is a combination of τ and τ_s.

This is the first important result of this paper. The rise time of the nonlinear effect due to a pulsed signal is governed merely by the signal pulse duration, while the fall time is a combination of the pulse duration and the response time of the EIT medium. This is in contrast to previous results [26,28] where step-response analysis was incorrectly generalized to draw conclusions about pulsed signal fields. An important implicit assumption of a step-response analysis in those cases is that the signal field remains on for a time longer than the response time of the system, an assumption that does not hold for pulsed signal fields.

In addition, the integrated phase shift per photon, ϕ_0, as predicted by the LTI model, Eq. (9), is seen to be independent of the signal pulse duration (recall that the energy of the signal pulse is held fixed). Importantly, the integrated phase shift scales inversely with the EIT window width for pumping rates much higher than the dephasing rate, $R \gg \gamma$; peaks when $R = \gamma$; and falls off for $R \ll \gamma$. The only other parameters that ϕ_0 depends on are the OD, d_0, the signal pulse detuning, Δ_s, and how tightly the signal beam is focused compared to the atomic cross section, $\sigma_{\rm at}/A$. We now turn to the dynamics of EIT-enhanced XPS and show that this linear model accurately predicts the behavior obtained from a numerical solution of the complete system density matrix.

III. RESULTS

In what follows, we show how different parameters of interest modify the behavior of EIT-enhanced XPS in the presence of a pulsed signal field. We consider both the numerical solution in Sec. II A and the LTI model in Sec. II B and show that the latter captures the salient features of this nonlinear interaction. We begin by discussing the effect of the transparency window width, $\Delta_{\rm EIT}$, on the XPS time response and the role that dephasing plays in this regard. In Sec. III B, we investigate the effects of the signal pulse duration and detuning, and we conclude by discussing in Sec. III C how an optically thick medium alters these dynamics. In order to carry out the numerical simulations, most of the medium parameters are chosen to be close to practically available values in a cold rubidium atom sample. However, it is important to remember that the qualitative results presented here are general properties of the N scheme regardless of the specific medium chosen to implement it.

A. Dependence on EIT medium properties

We first address how the width of the transparency window affects the dynamics of the EIT-enhanced XPS. In the original single-mode treatment, the size of the nonlinear phase shift

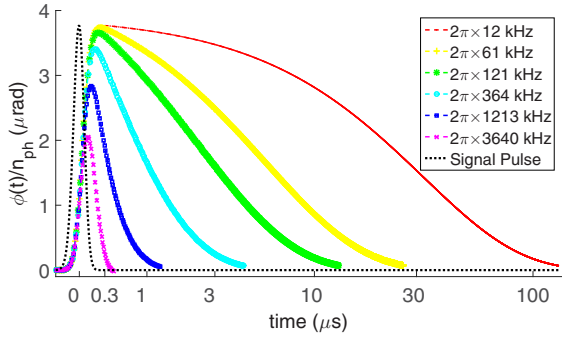

FIG. 2. Time dependence of the per-photon cross-phase shift for a variety of EIT window widths. The linear scaling of the peak XPS versus EIT window width breaks down once the response time of the EIT medium becomes comparable to or larger than the signal pulse duration. However, narrower window widths produce longer tails. Simulation parameters: $\Gamma = 2\pi \times 6$ MHz, $\tau_s = 1/2\sqrt{2}\pi \times 2000$ kHz^{-1}, $n_{\rm ph} = 100$, $d_0 = 1$, $\Delta_p = 0$, $\Delta_c = 0$, $\Delta_s = -10\Gamma$, $\sigma_{\rm at} = 1.2 \times 10^{-13}$ m^2, $\Omega_{0,p} = 0.003\Gamma$, $\gamma = 1 \times 10^{-5}\Gamma$, beam waist of 10 μm, and wavelength of 780.24 nm. The atomic cloud has a Gaussian spatial distribution. The legend shows the widths of the EIT windows used.

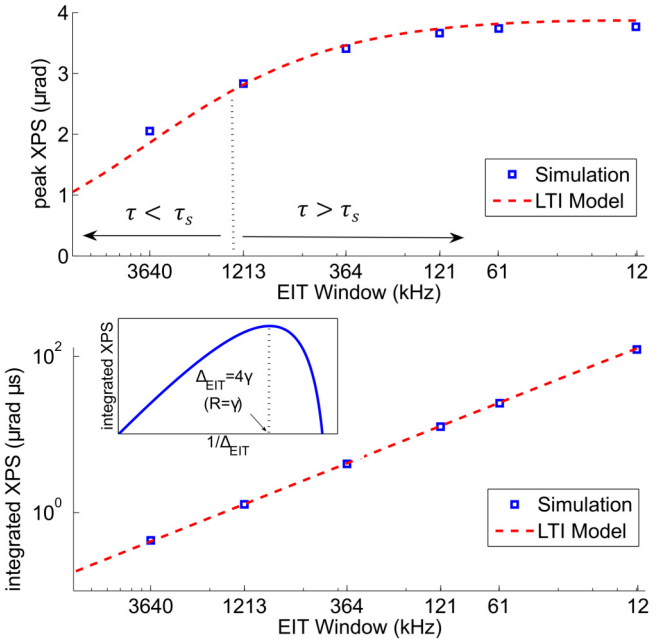

FIG. 3. Peak (top) and integrated (bottom) XPS per photon as extracted from Fig. 2. The peak XPS scales inversely with the EIT window only when the response time of the EIT medium is shorter than the signal pulse duration, while the integrated phase shift grows inversely with the window width owing to the longer tails that arise from narrower EIT windows. Squares correspond to simulation results and dashed lines show the prediction of the LTI model presented in Sec. II B. For window widths comparable to the natural linewidth of the transition the EIT medium response includes oscillations that are not included in the LTI impulse response, resulting in a small discrepancy between the two approaches. Also, the linear scaling of the integrated phase shift can be interrupted if the pumping and dephasing rates become comparable (inset).

increased indefinitely as the EIT window was narrowed. In the subsequent multimode, step-response analysis, the steady-state phase shift behaved similarly, but this steady state took longer to be established for narrower transparency windows. Figure 2 shows the temporal profile of the XPS experienced by a probe field in response to a Gaussian signal pulse for a variety of EIT window widths, as obtained by numerical simulation of Eq. (2). It is immediately evident that the rise time of the nonlinear phase shift is independent of the EIT window width, mimicking instead the rise of the signal pulse; also, as the window width narrows, the effect of the signal pulse on the probe field is prolonged. For narrower EIT windows, more time is required for the probe phase to return to its original steady-state value. For many practical applications of the EIT-enhanced cross-Kerr effect, this elongated tail permits a longer integration time and, hence, an improved signal-to-noise ratio.

Figure 3 shows the peak and integrated phase shifts extracted from Fig. 2 [(blue) squares] as well as those predicted from the LTI model in Sec. II B [dashed (red) line]. Immediately evident is the good agreement between these two approaches. In both cases, we see that the peak phase shift scales linearly with $1/\Delta_{\rm EIT}$ only when the EIT window is wide enough that $\tau \ll \tau_s$, i.e., when the response time is shorter than the signal pulse duration; once the window becomes narrower this linear scaling is disrupted, eventually plateauing for $\tau \gg \tau_s$. In fact, the peak phase shift changes by a mere factor of 2 for a window width variation that spans two orders of magnitude. Although the steady-state phase continues to grow with decreasing $\Delta_{\rm EIT}$, the time needed to reach this steady state also increases while the interaction time (signal pulse duration) is held constant here. Therefore, once $\Delta_{\rm EIT}$ is sufficiently narrow, decreasing the window width further does not help to increase the peak phase shift, which accounts for the plateau shown in Fig. 3. On the other hand, Fig. 3 also shows that the integrated phase continues to scale inversely with the EIT window width irrespective of the medium response time and the signal pulse duration. We are, therefore, led to conclude that the slow dynamics, far from degrading the effect, can still lead to an enhanced integrated XPS that could be exploited to obtain a better signal-to-noise ratio when detecting an EIT-based XPS, even when the peak phase shift saturates.

We see that the integrated phase shift scales as $1/\Delta_{\rm EIT}$ and this scaling is interrupted only by the ground-state dephasing rate, γ, which has only a technical, but no fundamental, limit. This dephasing limits the maximum depth of transparency, $d = d_0 R/(R+\gamma)$, as well as the minimum attainable EIT window width, $2(R+\gamma)$. These two quantities correspond to the rise and run, respectively, of the refractive index profile experienced by the probe field. Figure 4 shows the peak and integrated XPSs for various values of γ and a fixed pumping rate, R. The peak XPS falls by a factor of 2 at $\gamma = R$, while the integrated XPS does so at a value of γ smaller than R since it is affected by both the refractive index slope and the shortened tail.

Although current experimental efforts to achieve ever-narrower EIT windows are limited by dephasing rates, there is no fundamental limit to how low these dephasing rates can be. It is, therefore, important to understand whether there is a practical benefit to reducing dephasing given the potential limitations such as bandwidth and group velocity mismatch

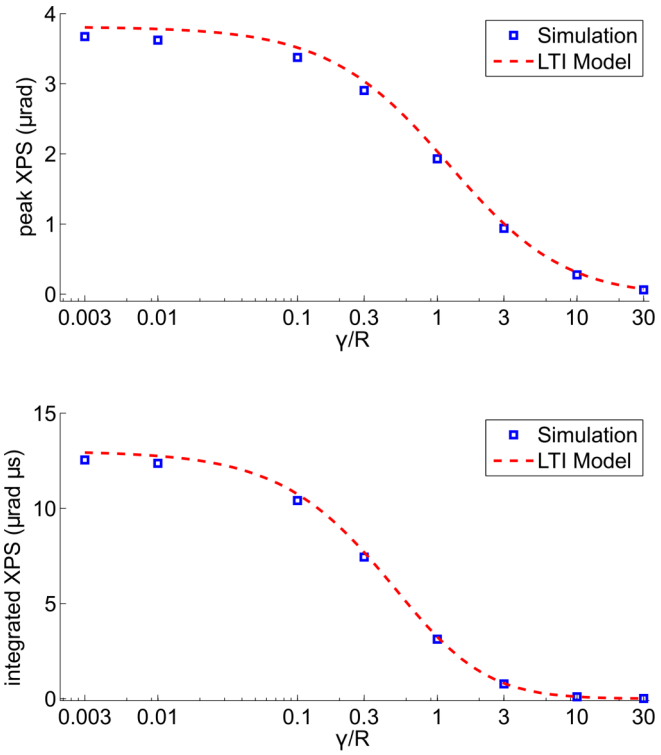

FIG. 4. Peak (top) and integrated (bottom) XPS per photon for various ground-state dephasing rates, γ. As the dephasing rate increases, both the peak and the integrated XPS decrease due to the degradation of the EIT window. The peak XPS falls to nearly half its ideal value when the dephasing rate becomes equal to the pumping rate, R. Squares correspond to simulation results, while dashed lines show the prediction of the LTI system response. For this simulation $R = 0.01\Gamma$, $\tau_s = (0.6\Gamma)^{-1}$, and the rest of parameters are the same as in Fig. 2. Note that the EIT window width is $2(R + \gamma)$.

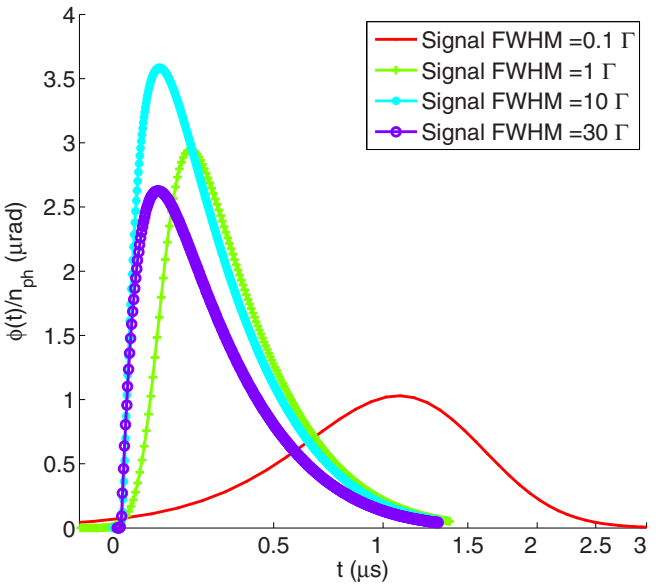

FIG. 5. Time response of XPS (per photon) for various signal pulse bandwidths. The linear scaling of the peak phase shift with signal pulse bandwidth breaks down when this bandwidth becomes comparable to or larger than the EIT window width. Once the bandwidth of the signal pulse becomes comparable to its detuning, $\Delta_s = -10\Gamma$, the peak XPS stops growing and starts to fall. Simulation parameters: $\Delta_{\mathrm{EIT}} = 0.2\Gamma$ and the rest of the parameters are the same as in Fig. 2.

brought about by narrower EIT windows. Therefore, for most of the results presented in this paper the dephasing rate is chosen to be negligibly small in order to study how different parameters of choice affect the behavior of the N scheme if we overcome the practical limitations imposed by dephasing.

B. Dependence on signal pulse

So far the only assumption we have made about the frequency content of the signal pulse is that its bandwidth is small compared to the signal pulse detuning. In this section we study how changing this frequency content can result in the modification of the behavior of the EIT-enhanced XPS. For simplicity, we assume that the signal pulse is transform limited, that is, that its bandwidth is proportional to $1/\tau_s$. Increasing the bandwidth, therefore, corresponds to a temporally shorter pulse. Since the Kerr effect depends linearly on the signal-field intensity, one would expect to be able to maximize the XPS, for a given pulse energy, by making the pulse as short, and therefore as intense, as possible. However, in the case where the spatial extent of the signal pulse is larger than the atomic medium, a shorter pulse yields a shorter interaction time and this must be weighed against the higher intensity due to broadening of the signal bandwidth (i.e., decreasing τ_s).

Figure 5 shows the temporal profile of the XPS for different signal pulse bandwidths for a constant pumping rate of $R = 0.1\Gamma$. We find that when $\tau_s \gg \tau$, the XPS replicates the temporal profile of the signal pulse but the peak phase shift is relatively small due to the low-intensity signal pulse. As one broadens the bandwidth of the pulse, the peak intensity and therefore the peak phase shift increase. However, this increase in peak phase shift with signal intensity is seen to saturate and even reverse once τ_s becomes sufficiently small. Figure 6 plots the peak and integrated XPS against the signal pulse bandwidth normalized to its detuning, Δ_s. For pulse bandwidths narrower than the EIT window the peak phase shift scales linearly with the signal bandwidth (and therefore linearly with the intensity) as expected from single-mode or step-response treatments. However, once the signal bandwidth exceeds the EIT window width, the scaling begins to flatten out. This saturation is a consequence of the trade-off between shorter interaction time and higher peak intensity of the signal pulse. Once the signal pulse has a bandwidth wider than the EIT window it exits the medium before the XPS reaches its peak value. Increasing the bandwidth further does not lead to a larger peak phase shift. The integrated XPS remains flat throughout all of this due to the fact that we have held the energy of the pulse and the window width constant.

Once the bandwidth of the signal pulse grows to be comparable to its detuning, the variation of the signal pulse amplitude versus the frequency becomes important. The response function used in Sec. II B does not take that frequency content into account and therefore fails to predict the behavior of the system properly. We can, however, qualitatively

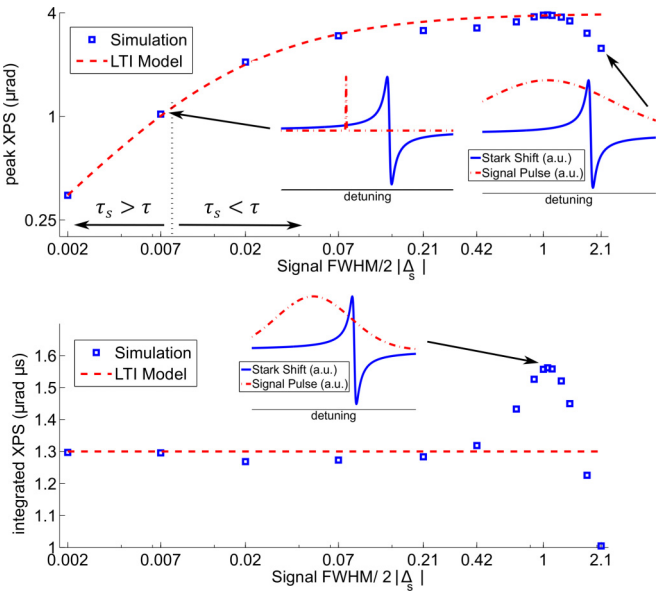

FIG. 6. Peak (top) and integrated (bottom) XPS per photon as a function of the signal-field bandwidth (normalized to central detuning) as extracted from Fig. 5. Initially, increasing the pulse bandwidth causes the peak XPS to grow proportionately due to the higher pulse intensity. However, once the pulse bandwidth becomes larger than the EIT window width, the peak XPS stops growing, similar to the behavior shown in Fig. 3. The maximum integrated XPS occurs when the pulse half-width at half-maximum of the intensity is equal to the detuning. Insets: The Fourier transform of the signal pulse intensity [dashed (red) line] along with the frequency dependence of the ac-Stark shift [solid (blue) line] as a function of the detuning from the excited state. For very broadband pulses, there is a discrepancy between the result of the LTI model and the numerical solution as explained in the text.

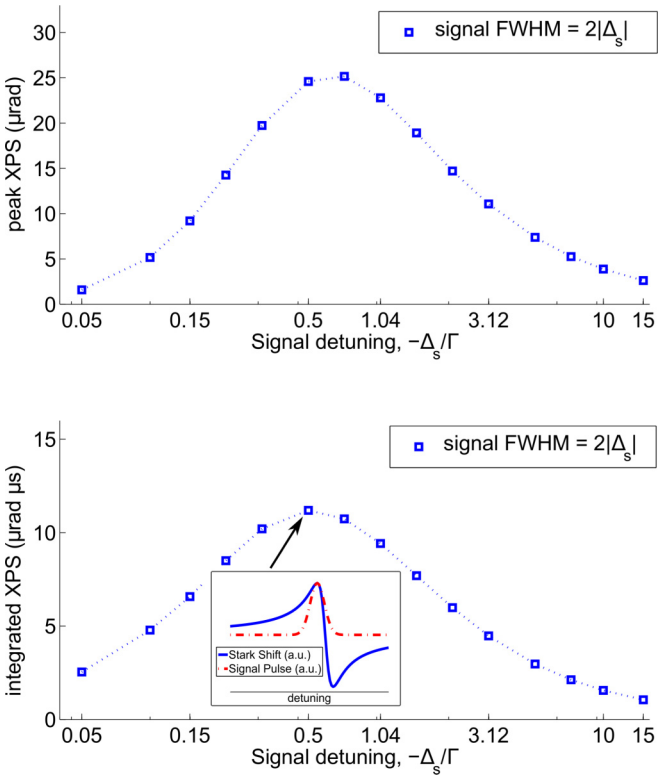

FIG. 7. Peak (top) and integrated (bottom) XPS per photon for various signal detunings, Δ_S, when the half-width at half-maximum of the signal pulse bandwidth is set equal to the detuning. Squares show simulation results, while the dotted line is a guide for the eye. Both the peak and the integrated XPS have maxima close to $\Delta_s = \Gamma/2$. Inset: The Fourier transform of the signal pulse intensity [dashed (red) line] along with the frequency dependence of the ac-Stark shift [solid (blue) line] as a function of the detuning from the excited state.

understand the behavior of XPS due to broadband pulses by recalling that the frequency dependence of the Stark effect resembles a refractive index profile. That is, it is an odd function passing though 0 on resonance, with extremes $\Gamma/2$ away on either side of resonance and scaling inversely with detuning away from resonance. Therefore, for a given signal pulse detuning, as its bandwidth is broadened, a point will be reached when frequency components begin to encroach on the peak of the Stark profile, leading to a larger XPS. However, as the bandwidth is broadened further, this increase is quickly reversed as the frequency components begin to cross over to the other side of the resonance addressed by this signal field. These frequency components then contribute strongly to the Stark shift but with opposite sign, yielding a smaller net phase shift. The optimum phase shift is obtained when the signal half-width at half-maximum (HWHM), $\sqrt{\ln 2}/\sqrt{2}\tau_s$, is equal to the signal detuning, Δ_s.

It is interesting to see how the XPS behaves as a function of the signal detuning when $\Delta_s\tau_s$ is held constant at the value of $\sqrt{\ln 2}/\sqrt{2}$. Figure 7 shows the peak and integrated XPS for the case where the signal HWHM is set equal to the detuning and then the two are varied simultaneously. It can be seen that the largest optimum phase shift is achieved close to $\Delta_s = \sqrt{\ln 2}/\sqrt{2}\tau_s = \Gamma/2$. For this choice of detuning and signal bandwidth the center of the pulse (in frequency space) coincides with the peak of the Stark shift frequency profile and its width covers those parts with the largest positive shift without spilling over onto the other side of the resonance (inset in Fig. 7).

C. Propagation in an optically thick medium

Thus far, we have neglected the effects that an optically thick medium would have on the dynamics of EIT-enhanced XPS. Steady-state analysis predicts that the XPS scales linearly with the OD and so it is of interest to see how the dynamics are affected by exploiting higher ODs. Particularly in the presence of EIT, which eliminates linear absorption, a higher OD increases the nonlinear interaction, with no detrimental effects arising from absorption. However, increasing the optical thickness of the medium also increases the difference in the group velocities of the probe and the signal pulses; the probe experiences a slow-light effect, while the signal field does not. This group velocity mismatch poses a limit on the maximum attainable peak phase shift as one increases the OD [31]. Given these trade-offs, here we discuss whether EIT-based XPS can still benefit from optically thick media.

In Refs. [27,28] the authors show that for the case of a step-function input field, the rise time depends linearly on

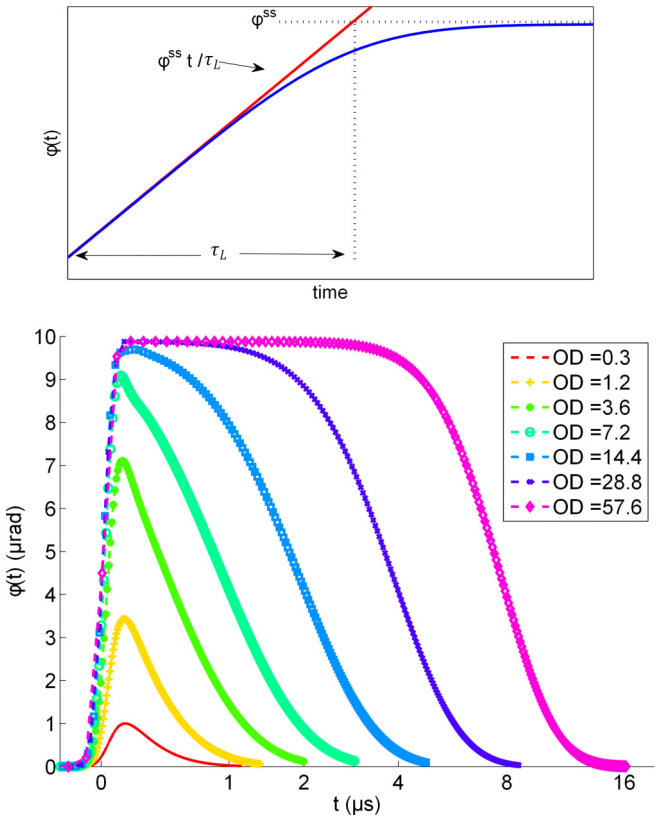

FIG. 8. XPS due to a step-function signal field (top) and time dependence of pulsed XPS (per photon) for different optical densities (bottom). As the optical density, d_0, increases the peak XPS begins to grow but eventually saturates due to the group velocity mismatch between the signal and the probe. However, higher values of the optical density result in longer-lasting phase shifts; the temporal extent of the flat region of the transient is determined by the duration of the probe that is compressed in the medium, τ_L, when the signal pulse passes through the medium at group velocity, c. Simulation parameters: $R = 0.1\Gamma$, $\tau_s = (0.6\Gamma)^{-1}$, and all others as in Fig. 2.

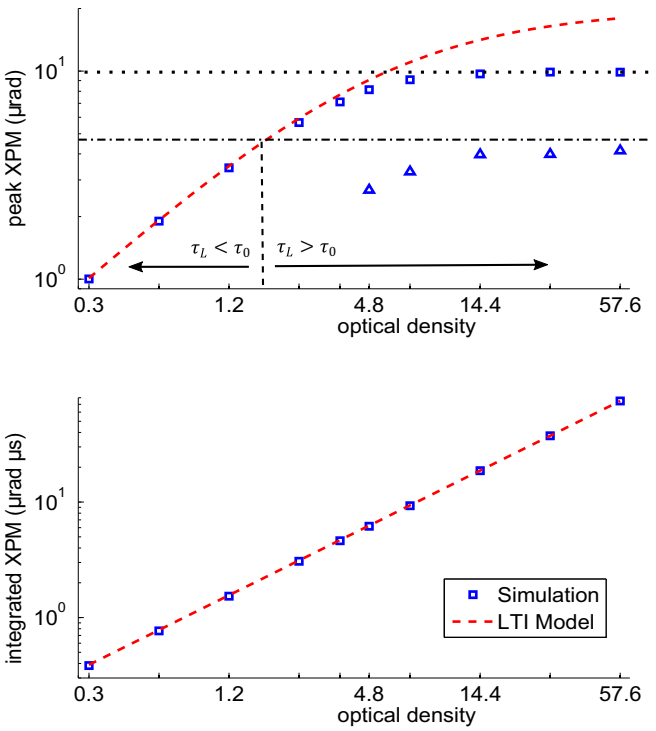

FIG. 9. Peak (top) and integrated (bottom) XPS per photon versus optical density, d_0, as extracted from Fig. 8. Squares correspond to simulation results, while dashed (red) lines are predictions of an LTI model. The response function adopted in Eq. (5) only partially accounts for the propagation effects (through the dependence of the EIT medium response time, τ, on the optical density); however, this is not sufficient to model the behavior of the system at high optical densities. This accounts for the discrepancy between the dashed (red) curve and the squares in the peak XPM plot. It is important to note that the response of the system is still linear at high optical densities and a proper impulse response can account completely for the saturation effect. The bottom plot shows that the integrated XPS increases linearly with the optical density and an LTI model agrees very well with the simulation results. τ_0 is the response time of the EIT medium in the limit of vanishing optical density. The dotted horizontal line in the top figure is the prediction given by Eq. (10) and the dashed-dotted horizontal line is the prediction from Ref. [31]. These two differ in the definition of the peak phase shift; the latter considers the phase of the probe at the peak of the signal pulse, while the former considers the probe phase once the entire signal pulse has passed through the medium. For comparison, the triangles show the value of the XPS as obtained from numerical simulation but using the definition of peak phase shift found in Ref. [31].

the OD. That result, however, does not directly hold for a pulsed signal. Here, we show that while the high OD results in a saturation of the peak phase shift due to group velocity mismatch [31], the peak value remains for a longer time for the higher OD.

For a sufficiently high OD, the transit time of the probe field through the sample becomes longer than the temporal duration of the signal pulse. In this case, there will be portions of the probe field inside the medium which experience the entire signal pulse as it passes through, and therefore, these portions acquire the maximum phase shift possible. The temporal length of this portion of the probe is equal to its group delay, $\tau_L = L/v_g = d_0(R - 2\gamma^2/\Gamma)/2(\gamma + R)^2$, where L is the length of the medium and v_g is the group velocity of the probe. This is reflected in Fig. 8, where we plot the temporal profiles of the XPSs for a variety of ODs. We see that for a high OD, the peak height of the phase shift plateaus but the duration of this peak XPS continues to grow as the OD is increased. Unlike the case of the response to a step signal, where the propagation effects show up in the rise time of the nonlinear phase shift [28], the response to a pulsed signal has a rise time determined by the signal pulse and the propagation effects only result in the saturation of the peak XPS in the time response. The net effect, as shown in Fig. 9, is such that while the peak phase shift saturates, the integrated phase shift scales linearly with OD.

To determine this saturation value of the peak XPS, it is instructive to consider the response of the system to a step signal [see Fig. 8 (top)], which includes a linear rise with time scale τ_L, followed by an exponential approach to the steady-state value. The slope of the rise, shown by the red line in Fig. 8 (top), is equal to $\frac{\phi^{ss}}{\tau_L}$. Since the impulse response is

the derivative of the step response, this slope determines the maximum achievable XPS for a pulsed signal in the presence of a high OD:

$$\phi_{\max} = \max\left\{\frac{\phi^{\rm ss}}{\tau_L}\Theta(t) * |\Omega_s(t)|^2\right\} = \frac{\phi^{\rm ss}}{\tau_L}\int_{-\infty}^{\infty} dt|\Omega_s(t)|^2 = n_{\rm ph}\frac{\Gamma}{-4\Delta_s}\frac{\sigma_{\rm at}}{A}. \quad (10)$$

This is a factor of 2 larger than the limit found by Harris and Hau due to group velocity mismatch in the N scheme [31]. In their work, with interactions between single-photon wave packets in mind, they assume that the probe and signal pulses have equal durations and enter the medium at the same time. They report the maximum achievable XPS at the location corresponding to the peak of the signal pulse. Since XPS is a cumulative effect, this assumption means that the acquired nonlinear phase shift is the result of the first half of the signal pulse. However, here we assume that the probe pulse can have a duration longer than the signal pulse and the maximum XPS is obtained only after the signal pulse has completely affected the probe. Figure 9 (top) shows the limit found by Harris and Hau (dashed-dotted horizontal line) and the limit found in Eq. (10) (dotted horizontal line). Values of the XPS obtained from numerical simulation at the location corresponding to the signal pulse peak are shown as triangles for comparison.

We also see that while the integrated phase shift is well modeled by our LTI approach, the peak phase shift is underestimated for sufficiently high ODs. This does not result from a breakdown of the linearity but, rather, because the response function assumed in Sec. II B did not account for such propagation effects. In an optically thick medium the effect from each thin slab of the medium takes some time, determined by the group velocity of the probe and the length of the medium, to reach the observer. Therefore, the exponential rise assumed in Eq. (3) does not capture the additional group delay effects present in media with high ODs.

IV. SUMMARY

We have studied the behavior of EIT-enhanced XPS for pulsed signals in the N scheme and shown how different parameters, such as the EIT window width, pulse bandwidth, and optical thickness, affect the transient behavior of the system. The results obtained here have important implications for quantum logic gates based on such EIT schemes. We have shown that, contrary to earlier fears about the finite response time, EIT may indeed be used to greatly enhance nonlinear phase shifts for applications such as quantum information processing. The importance of our work lies in the fact that previous studies have discussed only the steady-state or step-response scenarios rather than the realistic case of finite-duration pulses.

We have found that while the peak XPS is limited by the EIT response time and propagation effects, the integrated phase shift (a figure of merit not considered prior to this work) follows the prediction of the steady-state treatment. This integrated phase shift, which grows linearly with the OD and inversely with the EIT window width, is a more relevant figure of merit for the detectability of the XPS [4].

We have presented a treatment based on an LTI system response (taking the intensity of the signal as the "drive" and the phase shift on the probe as the "output") and shown that this adequately models the transient behavior of the Kerr XPS. While throughout the paper, we assume a Gaussian pulse shape for the signal, one should note that the exact shape of the signal pulse does not make a qualitative difference for the results presented.

The peak value and the duration of XPS are determined by several parameters, while the rise time of the effect is always dictated by the signal pulse duration. The peak XPS scales as the inverse of the EIT window width and is linear in pulse bandwidth as long as the EIT window is broader than the pulse bandwidth. However, for EIT windows narrower than the pulse bandwidth, even though there is no further increase in the peak XPS, the effect lasts for a longer time, providing more time for detecting the phase shift and potentially improving the signal-to-noise ratio. The peak XPS also scales linearly in OD as long as propagation effects can be neglected. For ODs above $\sim$2 (assuming negligible dephasing), the group velocity mismatch of the probe and the signal starts to play a significant role in the dynamics of the response and this poses a limitation on the maximum achievable peak phase shift. On the other hand, this group velocity mismatch causes the XPS to last longer. In short, narrow EIT windows and high ODs can enhance the detectability of XPS by elongating the duration of the effect.

For short signal pulses, when the bandwidth of the pulse becomes comparable to or larger than its detuning, it becomes necessary to take the frequency dependence of the Stark effect into account. Most importantly, the components of the signal pulse closer to the transition produce a larger Stark shift and consequently a stronger XPS. We have shown, using numerical solutions, that the optimum signal bandwidth is of the order of the signal detuning. The largest optimum XPS is achieved when both the detuning and the HWHM of the signal pulse are equal to the half-linewidth of the excited state.

The dependence on the EIT window and pulse duration of the rise and fall times, the peak phase shift, and the integrated phase shift has now been confirmed in an experiment we concluded after submission of the manuscript for this paper [32] and also used in an experimental observation of single-photon optical nonlinearity [33]. The present theoretical results make it promising to consider further extensions of that work, towards the regime of single-shot resolvability, as explained below. We have shown that the maximum achievable XPS value for a high OD is $\Gamma\sigma_{\rm at}/4\Delta_s A$ and that this value persists for a time $\tau_L = d/\Delta_{\rm EIT}$. One normally requires an EIT window that is narrower than the natural linewidth, $\Omega_c^2 < \Gamma^2$, and a probe field which is much weaker than the coupling field, say, $\Omega_p^2 = \zeta\Omega_c^2 < \zeta\Gamma^2$, where $\zeta \ll 1$. It is straightforward to show that a length τ_L of the probe field contains $\zeta\Gamma\tau_L A/\sigma_{\rm at} < \zeta A/\sigma_{\rm at}$ photons. Therefore the ratio of signal to quantum noise is

$$\frac{\Gamma}{4\Delta_s}\sqrt{\frac{\sigma_{\rm at}}{a}\zeta d}. \quad (11)$$

A beam size of 1 μm is achievable, which results in $\sigma_{\rm at}/A \approx 1/25$. To avoid signal absorption, one can operate farther from resonance, for example, at $\Delta_s = 2.5\Gamma$. ODs of 100 are typical in Bose-Einstein condensates and transient values of up to 1000 were observed in a dark-SPOT MOT

[34]. Since detectability is the only criterion here, one can use squeezed light to measure the phase of the probe. Quadrature squeezing around 10 dB has been observed [35]. Given such a set of (already experimentally achievable) parameters, one can obtain a signal-to-noise ratio of more than 1, in principle.

Note added in proof. Recently, developments using EIT systems, enhanced either by the use of a high-finesse cavity [36] or by the use of Rydberg transitions [37], have led to observations of per-photon phase shifts on the order of π.

ACKNOWLEDGMENTS

This work was funded by NSERC, CIFAR, Quantum Works, and Northrop-Grumman Aerospace Systems. We would like to thank Tilman Pfau for many stimulating discussions and for first raising the possibility that the finite response time of EIT might render the scheme invalid. We also thank Hamidreza Kaviani for discussions about the numerical methods.

[1] S. E. Harris and Y. Yamamoto, Phys. Rev. Lett. **81**, 3611 (1998).

[2] N. Imoto, H. A. Haus, and Y. Yamamoto, Phys. Rev. A **32**, 2287 (1985).

[3] D. Vitali, M. Fortunato, and P. Tombesi, Phys. Rev. Lett. **85**, 445 (2000).

[4] W. Munro, K. Nemoto, and T. Spiller, New J. Phys. **7**, 137 (2005).

[5] N. Matsuda, R. Shimizu, Y. Mitsumori, H. Kosaka, and K. Edamatsu, Nature Photon. **3**, 95 (2009).

[6] T. Peyronel, O. Firstenberg, Q.-Y. Liang, S. Hofferberth, A. V. Gorshkov, T. Pohl, M. D. Lukin, and V. Vuletić, Nature **488**, 57 (2012).

[7] O. Firstenberg, T. Peyronel, Q.-Y. Liang, A. V. Gorshkov, M. D. Lukin, and V. Vuletić, Nature **502**, 71 (2013).

[8] W. Chen, K. M. Beck, R. Bücker, M. Gullans, M. D. Lukin, H. Tanji-Suzuki, and V. Vuletić, Science **341**, 768 (2013); http://www.sciencemag.org/content/341/6147/768.full.pdf.

[9] S. Baur, D. Tiarks, G. Rempe, and S. Dürr, Phys. Rev. Lett. **112**, 073901 (2014).

[10] V. Venkataraman, K. Saha, and A. L. Gaeta, Nature Photon. **7**, 138 (2013).

[11] D. O'Shea, C. Junge, J. Volz, and A. Rauschenbeutel, Phys. Rev. Lett. **111**, 193601 (2013).

[12] A. Feizpour, X. Xing, and A. M. Steinberg, Phys. Rev. Lett. **107**, 133603 (2011).

[13] H. Schmidt and A. Imamoglu, Opt. Lett. **21**, 1936 (1996).

[14] M. Fleischhauer, A. Imamoglu, and J. Marangos, Rev. Mod. Phys. **77**, 633 (2005).

[15] D. A. Braje, V. Balić, G. Y. Yin, and S. E. Harris, Phys. Rev. A **68**, 041801 (2003).

[16] H. Kang and Y. Zhu, Phys. Rev. Lett. **91**, 093601 (2003).

[17] H.-Y. Lo, Y.-C. Chen, P.-C. Su, H.-C. Chen, J.-X. Chen, Y.-C. Chen, I. A. Yu, and Y.-F. Chen, Phys. Rev. A **83**, 041804 (2011).

[18] H. X. Chen, A. V. Durrant, J. P. Marangos, and J. A. Vaccaro, Phys. Rev. A **58**, 1545 (1998).

[19] Y. Li and M. Xiao, Opt. Lett. **20**, 1489 (1995).

[20] A. Godone, S. Micalizio, and F. Levi, Phys. Rev. A **66**, 063807 (2002).

[21] S. J. Park, H. Cho, T. Y. Kwon, and H. S. Lee, Phys. Rev. A **69**, 023806 (2004).

[22] Y.-F. Chen, G.-C. Pan, and I. A. Yu, Phys. Rev. A **69**, 063801 (2004).

[23] J. Shen, Z. Ruan, and S. He, Phys. Lett. A **330**, 487 (2004).

[24] H. Schmidt and A. Imamoğlu, Opt. Lett. **23**, 1007 (1998).

[25] L. Deng, M. G. Payne, and W. R. Garrett, Phys. Rev. A **64**, 023807 (2001).

[26] G. F. Sinclair, Phys. Rev. A **79**, 023815 (2009).

[27] M. V. Pack, R. M. Camacho, and J. C. Howell, Phys. Rev. A **74**, 013812 (2006).

[28] M. V. Pack, R. M. Camacho, and J. C. Howell, Phys. Rev. A **76**, 033835 (2007).

[29] G. J. Milburn, Phys. Rev. Lett. **62**, 2124 (1989).

[30] C. L. Philips, J. M. Parr, and E. Riskin, *Signals, Systems, and Transforms* (Prentice Hall, Upper Saddle River, NJ, 1995).

[31] S. E. Harris and L. V. Hau, Phys. Rev. Lett. **82**, 4611 (1999).

[32] G. Dmochowski, A. Feizpour, M. Hallaji, C. Zhuang, A. Hayat, and A. Steinberg, arXiv:1506.07051.

[33] A. Feizpour, M. Hallaji, G. Dmochowski, and A. M. Steinberg, Nature Phys. **11**, 905 (2015).

[34] B. M. Sparkes, J. Bernu, M. Hosseini, J. Geng, Q. Glorieux, P. A. Altin, P. K. Lam, N. P. Robins, and B. C. Buchler, J. Phys.: Conf. Ser. **467**, 012009 (2013).

[35] Y. Takeno, M. Yukawa, H. Yonezawa, and A. Furusawa, Opt. Express **15**, 4321 (2007).

[36] K. M. Beck, M. Hosseini, Y. Duan, and V. Vuletić, arXiv:1512.02166 (2015).

[37] D. Tiarks, S. Schmidt, G. Rempe, and S. Dürr, arXiv:1512.05740 (2015).